NESTOR Shielding and Dosimetry Improvement Programme.

The ASPIS-PCA Slab Geometry Benchmarks.

Blind Test Edition.

M D Carter
I J Curl

UK ATOMIC ENERGY AUTHORITY

WINFRITH

Reactor Physics Division
June 1986

CORRIGENDA TO AEEW - M 2329

Check measurements have been made on the NESDIP 1 and 2 arrays as part of a series of reproducibility tests on the NESDIP series of experiments. These have shown that the plate, representing the stainless steel thermal baffle, was manufactured to a thickness of 6.3 cm and not to the specified thickness of 5.9 cm. Regrettably this was not noticed during the engineering acceptance tests and the 'as drawn' thickness of 5.9 cm was mistakenly included in this report. All other dimensions given in the report are correct.

The following changes should be made to the document.

Page 2

Table 2.1 'Thermal Baffle 5.9' change to 'Thermal Baffle 6.3'

Table 2.2 'Thermal Baffle 5.9' change to 'Thermal Baffle 6.3'

Section 2, Item 3.
'which contains the 5.9 cm thick Stainless Steel plate' change to
'which contains the 6.3 cm thick Stainless Steel Plate'.

Page 12

Figure 6.1 Distances from inside face of trolley front should change to
... 66.2, 78.3, **84.6, 97,8, 100.3, 120.6, 150.2, 152.1, 174.5, 180.0,** 200.0

Figure 6.2 Distances from inside face of trolley front should change to
... 65.5, 77.6, **83.9, 97.1, 99.6, 119.9, 147.9, 149.8, 172.2, 174.7,** 200.0

Abstract

The ASPIS-PCA slab geometry benchmark experiments comprise Phase 2 of the NESTOR Shielding and Dosimetry Improvement Programme, NESDIP (10). The experimental configurations are an extension of the PCA REPLICA which was a replication in the ASPIS facility at AEE Winfrith of the 12/13 configuration of the ORNL PCA. The restricted lateral dimensions of the PCA and REPLICA configurations (685x685mm) are not well suited to solution using one- and two-dimensional codes and the present studies have been carried out using shield components of 1829x1910mm cross-section.

The paper provides a detailed summary of the experimental configurations. The fission plate sources are described with notes on their calibration. Measurements were made using threshold reaction-rate detectors and the locations of these detectors are given. The paper does not provide the absolute calibration of the source or the results of the threshold measurements. The results have been replaced in this edition of the paper by the symbol xxxxx in order that the experiments can be used as a blind test of calculational methods.

The experimental results will be made available in the second edition of this paper. This will also include our analysis of the data using the Monte Carlo code MCBEND.

Reactor Physics Division
AEE Winfrith

June 1986

Contents

Contents (continued)

Appendices (not included in this edition)

Tables

Contents (continued)

Figures

1 · Introduction

The NESTOR shielding and Dosimetry Improvement Programme NESDIP was conceived to study neutron penetration through typical PWR radial shields. The programme encompasses both penetration through the radial shield from the core boundary to the cavity external to the reactor pressure vessel and the subsequent transport within the cavity. The first 3 Phases of NESDIP study the radial penetration to the cavity and Phases 4 and 5 study streaming within the cavity and in a simulated nozzle and coolant duct configuration.

In Phase 1 of NESDIP an exact replica of the American PCA radial shield benchmark (1) was constructed in a large water tank mounted in the ASPIS trolley in order to investigate discrepancies in the PCA between measurement and calculation. The REPLICA configuration is shown in Figure 1.1. The first part of the analysis of this experiment has been reported in Reference 1.

The second phase of NESDIP, with which this report is concerned, is a natural extension of the PCA and REPLICA experiments whereby the lateral extent of the configuration is expanded to fill the full height and width of the ASPIS trolley. The PCA configuration is thereby represented by a combination of slabs and water tanks of 1829mm x 1910mm cross-sectional area, the thickness of each region ideally remaining unchanged; in practice two minor dimensional changes have been made, these are discussed in Section 2. To fulfil a major concept of the NESDIP studies the move away from the REPLICA configuration is carried out in well defined stages. In this phase of NESDIP two series of measurements have been conducted. The first series retains the small rectangular fission plate used in the REPLICA experiment; for historical reasons this configuration is known as the NESDIP 1 radial shield. The second series utilises a large circular fission plate with an effective radius of 56cm; this configuration is known as the NESDIP 2 radial shield. Both configurations have common slab components aft of their respective fission plates. With a spatially large source, as in the NESDIP 2 configuration the effect of the lateral leakage on the centre-line fluxes is substantially reduced and the geometry of the system can be adequately represented by two-dimensional RZ models. The two geometric configurations studied in this phase of NESDIP are shown relative to the REPLICA configuration in Figure 1.

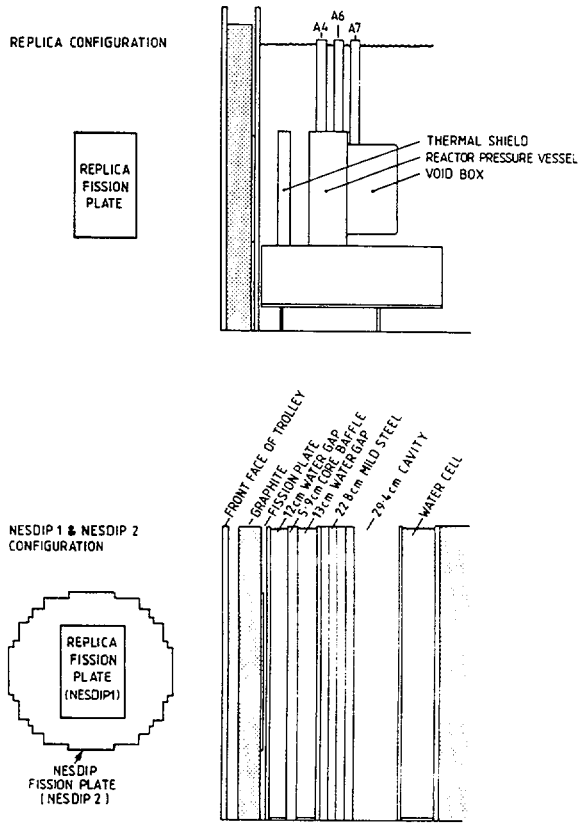

Figure 1.1 *The REPLICA and the Aspis PCA slab geometry benchmarks*

The data presented in the first 4 sections of this report, specifically the geometric configurations, (Section 2), neutron source distributions (Section 3) and measurement details (Sections 4 and 5) are sufficient to enable calculations to be performed for a unit power of 1 watt in the fission plate. The Blind Test format of this report is such that the absolute power of the fission plate and the results of the experimental results have been omitted. All censored data has been replaced by xxxxx. Statistical uncertainties (1) have been included to show the quality of data to be presented. Section 6 is a skeletal account of the Winfrith analysis using Monte Carlo Methods. It has been included as an aid to understanding.

All omitted results and comparisons will be included in the second editon of this paper.

2 The experimental configurations

The transformation of the REPLICA configuration to a 1829mm × 1910mm slab representation has been governed by the following considerations.

1 To allow the use of stock components the mild steel block, representing the pressure vessel was constructed from four 5.08cm thick plates and the 2.5cm plate which forms the rear wall of the water cell. Hence the total steel thickness is 22.8cm. This compares with the thickness of the PCA mild steel block which was 22.5cm.

2 In addition to measurements in the shield, the roof slot of the ASPIS facility was to be used to extend the cavity region above the height of the trolley so that streaming measurements could be conducted. This placed a constraint on the positioning of the array within the trolley in order that the front (NESTOR side) face of the cavity aligned with the front face of the roof slot. The whole shield configuration was therefore moved 7.9cm further from the front of the trolley than in the REPLICA experiment. In doing so the absolute power of the fission plate is reduced but the relative neutron distribution is virtually unaffected.

3 The water cells bow when filled. The 12/13 configuration is constructed from a single water tank which contains the 5.9cm thick stainless steel thermal baffle. The baffle is located to maintain the front water gap at 12.1cm and the expansion due to bowing is taken up in the rear water compartment which has a thickness of 13.2cm, 5mm greater than in the REPLICA experiment.

In addition differences exist between the NESDIP 1 and NESDIP 2 arrays due to the different types of fission plate used and their mountings.

The dimensions of both the NESDIP 1 and 2 configurations are given in Tables 2.1 and 2.2 respectively. The material specifications are given in Table 2.4. In both configurations the geometric centre of the fuelled region of each fission plate is located at the nuclear centre of the trolley. The location of the nuclear centre relative to the internal surfaces of the trolley is shown in Figure 3.5 where it can be seen that it is only slightly displaced from the geometric centre of the trolley.

Details of spot measurements of the front and rear water gaps are presented in Table 2.3.

Table 2.1 Dimensions and materials in the NESDIP 1 array

Assembly	Component	Thickness (cm)	Material	Material Reference No*
Trolley Face		3.2	Mild Steel with Aluminium Window of radius 56.1cm	3&8
Void		7.9	—	0
Graphite		15.0	Graphite	1
Void		1.9	—	0
Fission Plate	Coverplate	0.4	Aluminium	9
	Void	0.1	—	0
	Fuel	0.4	Fuel	7
	Void	0.1	—	0
	Coverplate	0.4	Aluminium	9
Water Cell No 1	Front Face	1.9	Aluminium	9
	Water Gap	12.1**	Water	10
	Thermal Baffle	5.9	Stainless Steel	6
	Water Gap	13.2**	Water	10
	Rear Face	2.5	Mild Steel	4
RPV	Plate 1	5.1***	Mild Steel	5
	Plate 2	5.1***	Mild Steel	5
	Plate 3	5.1***	Mild Steel	5
	Plate 4	5.1***	Mild Steel	5
Cavity		29.6	—	0
Water Cell No 2	Front Face	1.9	Aluminium	9
	Water Gap	22.5	Water	10
	Rear Face	2.5	Mild Steel	5
Biological Shield		61.0	Concrete	2

*Reference Table 2.4

**This dimension is greater than the specification due to cell bowing

***A 0.6cm void was opened up in front of this component for activation foil measurements

Note: With the exception of the fission plate all shield components are 191.0cm high and 182.9cm wide. The fission plate is 68.5cm high and 47.5cm wide.

Table 2.2 Dimensions and materials in the NESDIP 2 array

Assembly	Component	Thickness (cm)	Material	Material Reference No*
Trolley Face		3.2	Mild Steel with Aluminium Window of radius 56.1cm	3&8
Void		6.0	—	0
Graphite		15.0	Graphite	1
Void		1.2	—	0
Fission Plate	Coverplate	1.2	Aluminium	9
	Void	0.1	—	0
	Blank	0.1	Aluminium	9
	Fuel	0.2	Fuel	7
	Blank	0.1	Aluminium	9
	Coverplate	1.2	Aluminium	9
Void		0.4	—	0
Water Cell No 1	Front Face	1.9	Aluminium	9
	Water Gap	12.1**	Water	10
	Thermal Baffle	5.9	Stainless Steel	6
	Water Gap	13.2**	Water	10
	Rear Face	2.5	Mild Steel	4
RPV	Plate 1	5.1***	Mild Steel	5
	Plate 2	5.1***	Mild Steel	5
	Plate 3	5.1***	Mild Steel	5
	Plate 4	5.1***	Mild Steel	5
Cavity		29.4	—	0
Water Cell No 2	Front Face	1.9	Aluminium	9
	Water Gap	22.5	Water	10
	Rear Face	2.5	Mild Steel	5
Biological Shield		61.0	Concrete	2

*Reference Table 2.4

**This dimension is greater than the specification due to cell bowing

***A 0.6cm void was opened up in front of this component for activation foil measurements

Note: All shield components are 191.0 cm high and 182.9cm wide.

3 The fission plates

Table 2.3 Measurement of water gaps

Y Co-ordinate	Front Water Gap			Rear Water Gap		
	X co-ordinate (cm)			X co-ordinate (cm)		
(cm)	−20	0	20	−20	0	20
20	11.99	12.04	11.98	13.57	13.52	13.34
0	12.17	12.21	12.13	13.26	13.16	13.04
−20	11.96	12.00	11.94	13.31	13.25	13.13

Table 2.4 Material compositions

Material	Material Reference* No.	Density	Element	Atom Fraction
GRAPHITE	1	1.650	C	1.0000
CONCRETE	2	2.300	Si	0.2044
			Fe	0.0043
			H	0.1690
			O	0.5633
			Al	0.0215
			Ca	0.0161
			Na	0.0119
			K	0.0096
MILD STEEL	3	7.835	Fe	0.9781
			Mn	0.0110
			C	0.0102
			Si	0.0007
MILD STEEL	4	7.862	Fe	0.9958
			Mn	0.0024
			C	0.0018
MILD STEEL	5	7.850	Fe	0.9816
			Mn	0.0075
			C	0.0106
			H	0.0003
STAINLESS STEEL	6	7.900	Fe	0.6914
			C	0.0011
			Ni	0.0934
			Cr	0.1856
			Ti	0.0021
			Si	0.0121
			Mn	0.0143
FUEL	7	3.256	Al	0.9721
			U235	0.0260
			U238	0.0019
ALUMINIUM	8	2.700	Al	1.0000
ALUMINIUM	9	2.666	Al	0.9959
			Si	0.0014
			Fe	0.0027
WATER	10	1.000	H	0.6667
			O	0.3333

*Reference Tables 2.1 and 2.2

Two fission plates have been used in this phase of NESDIP. The small rectangular fission plate manufactured for the REPLICA experiment was used in the NESDIP 1 configuration and a large circular fission plate, the NESDIP fission plate was used in the NESDIP 2 configuration.

3.1 The REPLICA Fission-Plate

The REPLICA fission-plate is constructed of 52 uranium aluminium alloy fuel strips of height 635mm, width 30.48mm and thickness 1.016mm. The strips, of density 3.256g.cm^{-3}, are 80% by weight of Al and 20% by weight of U enriched to 93%. Sets of 4 fuel strips are laid on top of each other and 13 of these assemblies are placed side by side on a pitch of 30.92mm to form the fuel structure of the fission plate. This structure is enclosed in a thin aluminium envelope. The fission-plate is shown schematically in Figure 3.1.

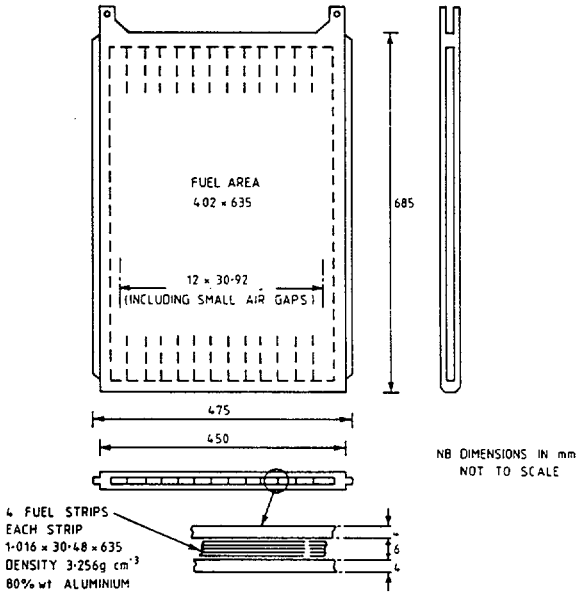

Figure 3.1 *The REPLICA fission plate*

The full calibration procedure for fission plates was originally described in the REPLICA report (1). In summary the calibration divides into two parts; the first is the determination of the relative fission-rate distribution over the plate from measurement of Mn55(n,γ)Mn56 reaction-rates made on the front face of the plate. In the second part the relative fission-rate profile is normalised to absolute measurements of the fission-rate, per NESTOR watt, in the plate. The full procedure is contained in Section 3.2 as part of the calibration of the large circular NESDIP fission plate.

By design there is a very high degree of similarity in the environment surounding the fission plate in the REPLICA and NESDIP 1 configurations. Hence the power distribution profile over the plate in the two situations were not expected to be significantly different. The absolute power of the plate in the NESDIP 1 configuration was however expected to drop relative to the REPLICA configuration due to the repositioning of the shield further back into the trolley. The relative power profile of the plate in NESDIP 1 was established in the usual manner using measured Mn55(n,γ)Mn56 reaction-rate data and the source definition programe CRISP (2). The resulting power profile is shown in Figure 3.2 and the neutron source strengths per Watt of plate power ($n.cm^{-3}s^{-1}$) for the demonstration source mesh used in the REPLICA report are given in Table 3.1.

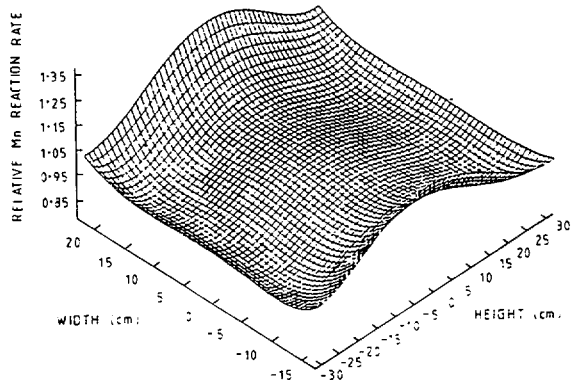

Figure 3.2 *The source profile of the REPLICA fission plate in the NESDIP 1 array.*

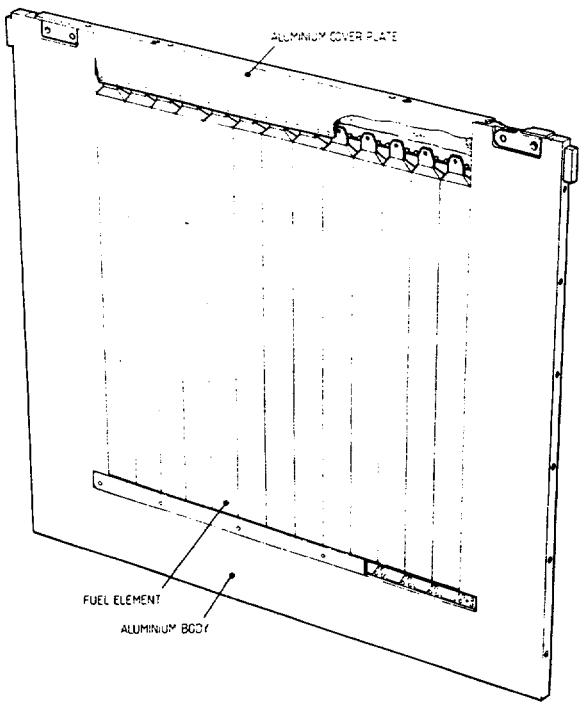

Figure 3.3 *The NESDIP fission plate*

During all irradiations of activation detectors within the shield, three sulphur pellets were placed in locations at the centre of the front face of the fission plate to monitor the local fast flux, via the S32(n,p)P32 reaction; the prime aim being to guard against human error in recording the irradiation time or indicated power. They also provide a measure of the local fission-rate within the plate which can be used to scale the plate power in this Phase of the work from its calibrated value in the REPLICA configuration of 6.74×10^{-4} ($\pm 3.6\%$) Watts per NESTOR Watt.

The sulphur monitor reaction-rates are assumed proportional to the local fission-rate at the centre of the plate. To use the sulphur monitors as a measurement of the average fission plate power over the whole plate each sulphur measurement is adjusted by the ratio, A, of the fission-rate at the centre of the plate to the average fission-rate over the whole plate. The ratio A is derived during the definition of the fission-rate profile as part of the analysis by the CRISP code (2). The scaling of the REPLICA calibration by the ratio of the adjusted sulphur reaction rates at the monitor position yields the plate power R, per NESTOR watt, in the NESDIP 1 configuration:

$$R = 6.74, -4\,(\pm 3.6\%) \times \frac{A_R}{S_R} \times \frac{S_1}{A_1}$$

where S_R = sulphur monitor reaction-rate per NESTOR Watt in the REPLICA configuration

= 2.443, −21 d.p.s.atom^{-1} per NESTOR watt ($\pm 0.7\%$: counting statistic)

S_1 = sulphur monitor reaction-rate per NESTOR watt in the NESDIP 1 configuration

= XXXXX d.p.s.atom^{-1} per NESTOR watt ($\pm 0.7\%$: counting statistic)

A_R = centre/average fission-rate ratio for the REPLICA configuration

= 1.058 ($\pm 1\%$)

A_1 = centre/average fission-rate ratio for the NESDIP 1 configuration

= 1.035 ($\pm 1\%$)

Hence R = XXXXX ($\pm 4.0\%$) Watts

3.2 The NESDIP Fission Plate

The NESDIP fission plate is shown in Figure 3.3. It comprises an aluminium frame which fills the height and width of the ASPIS trolley. Located within the frame are 13 separate fuel elements. An exploded view of an individual fuel element is shown in Figure 3.4. Each element has two 12mm thick aluminium cover plates which attach on either side of the top and bottom locating end pieces leaving a 5mm separation in which U/Al alloy fuel strips are located. The fuel strips are of the same type as used in the REPLICA plate, i.e. of density 3.256g.cm^{-3}, are 80% by weight of Al and 20% by weight of U enriched to 93%. They are nominally 30.5mm wide and 1mm thick and are screwed to the rear cover plate.

Table 3.1 Source distribution in the REPLICA fission plate in the NESDIP 1 array

Y co-ordinates (cm) \ X-coordinates (cm)	−20.10 to −12.10	−4.10	4.10	12.10	20.10
31.75	4.911E+7	4.770E+7	4.739E+7	4.681E+7	4.846E+7
26.32	4.886E+7	4.670E+7	4.634E+7	4.583E+7	4.892E+7
20.58	5.041E+7	4.753E+7	4.723E+7	4.682E+7	5.066E+7
15.44	5.251E+7	4.904E+7	4.886E+7	4.849E+7	5.264E+7
10.00	5.455E+7	5.059E+7	5.057E+7	5.018E+7	5.435E+7
3.33	5.562E+7	5.124E+7	5.141E+7	5.093E+7	5.485E+7
−3.33	5.509E+7	5.041E+7	5.073E+7	5.021E+7	5.367E+7
−10.00	5.346E+7	4.864E+7	4.905E+7	4.856E+7	5.149E+7
−15.44	5.158E+7	4.690E+7	4.734E+7	4.693E+7	4.993E+7
−20.58	4.990E+7	4.592E+7	4.632E+7	4.601E+7	4.785E+7
−26.32	4.935E+7	4.715E+7	4.741E+7	4.701E+7	4.842E+7
−31.75					

Notes

1. Table values are in units of neutrons.cm^{-3} per plate Watt
2. The fuelled area of the plate is taken as 6mm thick
3. The fission rate profile through the fuel is reproduced below from Reference 1

Fuel Spike	Relative Profile
1	1.109±0.008
2	0.997±0.027
3	0.939±0.020
4	0.955±0.013
Mean 1 to 4	1.00 ±0.006

Spike 1 is closest to NESTOR core

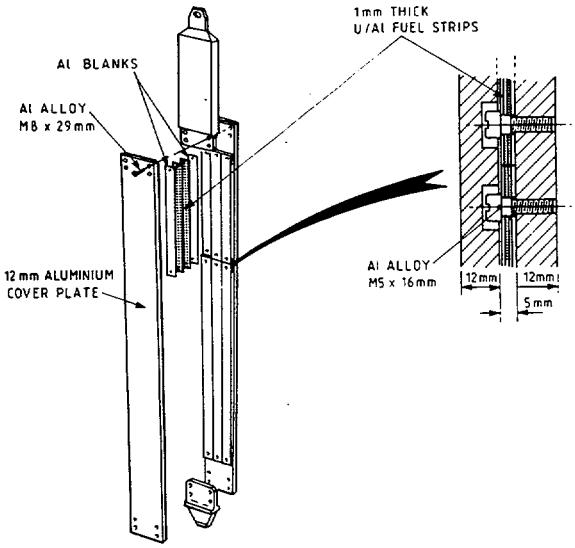

Figure 3.4 *Aspis U/AL alloy fuel element*

Table 3.2 Source distribution in the NESDIP fission plate in the NESDIP 2 array

ANNULAR

Outer Radius (cm)	Source* (n.cm^{-3}.s^{-1})Plate Watt
0	
5	6.16.7
10	6.13.7
15	5.92.7
20	5.65.7
25	5.42.7
30	5.04.7
35	4.66.7
40	4.21.7
45	3.81.7
50	3.41.7
56.5	1.18.7

*Note the source data given are averaged values for each annular source region.

RECTANGULAR

	-52.25	-49.08	-45.92	-39.58	-36.42	-30.08	-14.25	-4.75	4.75	14.25	30.08	36.42	39.58	45.92	49.08	52
51.44....	0	0	0	0	0	0	3.236,7	3.277,7	3.236,7	0	0	0	0	0	0	
47.63....	0	0	0	0	0	3.333,7	3.572,7	3.642,7	3.591,7	3.327,7	0	0	0	0	0	
40.64....	0	0	0	0	3.323,7	3.693,7	4.021,7	4.115,7	4.052,7	3.711,7	3.245,7	0	0	0	0	
35.56....	0	0	0	3.356,7	3.551,7	3.994,7	4.375,7	4.484,7	4.412,7	4.022,7	3.483,7	3.205,7	0	0	0	
31.75....	0	0	3.489,7	3.729,7	3.983,7	4.531,7	4.985,7	5.110,7	5.022,7	4.561,7	3.921,7	3.587,7	3.231,7	0	0	
19.69....	0	3.502,7	3.784,7	4.079,7	4.380,7	5.009,7	5.517,7	5.651,7	5.549,7	5.032,7	4.317,7	3.941,7	3.539,7	3.125,7	0	
15.88....	3.447,7	3.651,7	3.973,7	4.302,7	4.632,7	5.307,7	5.842,7	5.977,7	5.861,7	5.316,7	4.562,7	4.166,7	3.741,7	3.304,7	3.011,7	
5.29....	3.482,7	3.713,7	4.070,7	4.428,7	4.779,7	5.484,7	6.029,7	6.159,7	6.035,7	5.468,7	4.697,7	4.295,7	3.866,7	3.425,7	3.129,7	
-5.29....	3.319,7	3.553,7	3.910,7	4.264,7	4.610,7	5.296,7	5.819,7	5.937,7	5.808,7	5.255,7	4.518,7	4.139,7	3.738,7	3.331,7	3.062,7	
-15.88....	0	3.335,7	3.672,7	4.007,7	4.334,7	4.982,7	5.472,7	5.578,7	5.450,7	4.926,7	4.238,7	3.889,7	3.524,7	3.159,7	0	
-19.69....	0	0	3.309,7	3.603,7	3.891,7	4.465,7	4.898,7	4.986,7	4.866,7	4.393,7	3.789,7	3.489,7	3.183,7	0	0	
-31.75....	0	0	0	3.157,7	3.393,7	3.869,7	4.228,7	4.296,7	4.186,7	3.782,7	3.282,7	3.043,7	0	0	0	
-35.56....	0	0	0	0	3.113,7	3.518,7	3.825,7	3.880,7	3.779,7	3.423,7	2.994,7	0	0	0	0	
-40.64....	0	0	0	0	0	3.071,7	3.296,7	3.330,7	3.243,7	2.963,7	0	0	0	0	0	
-47.63....	0	0	0	0	0	0	2.870,7	2.883,7	2.811,7	0	0	0	0	0	0	
-51.44....																

Fuelled region is 2mm thick

There is depth for 4 fuel strips within each element leaving a 1mm clearance gap next to the front cover plate. Three columns of fuel strips laid side by side fill the width of the element. In the NESDIP configuration only the central two strips in each column contain U/Al alloy, the outer two are both blanks manufactured from aluminium. To approximate to a disc fission neutron source the axial fuel loading within each element has been arranged to the specification of Figure 3.5 and 3.9 by the substitution of aluminium blanks where necessary.

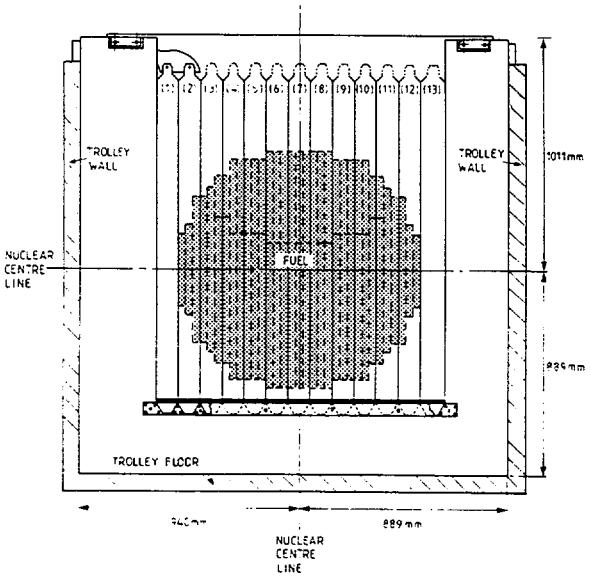

Figure 3.5 *Detail of fuel loading pattern when viewed looking towards the NESTOR core*

3.2.1 The Fission-Rate Distribution within the NESDIP Fission Plate Located in the NESDIP 2 Radial Shield Array

The approach taken to obtain the absolute power distribution throughout the fission plate in this Phase of NESDIP follows the procedure set out in the NESDIP Replica Experiment. In summary the procedure is as follows:

(1) The measurement of manganese reaction-rates over the front surface of the fission plate to define a thermal flux profile in X and Y (coordinate system defined in Figure 3.6);

(2) A measurement of the distribution of the U235 content within the fuel;

(3) Combining (1) and (2) to provide a relative fission-rate profile in X and Y;

(4) The definition of a relative fission profile in the Z direction through the fuel from fission product decay measurement of irradiated fuel;

(5) Normalisation of the fission-rate profile to absolute measurements of the fission-rate per NESTOR Watt in the plate.

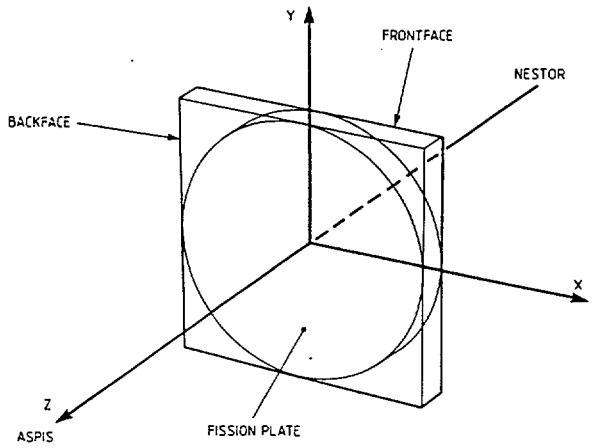

Figure 3.6 *Co-ordinate system*

3.2.2 The Low-Energy Neutron Flux Profile Over the Fission Plate

Measurements of the Mn55(n.γ)Mn56 reaction-rate on the front and back faces of the fission plate were made with 12.7mm diameter Mn foils. The distribution of foils on the front face of the fission plate is shown in Figure 3.7. The foils on the back face were positioned directly behind the foils on the front face marked by an asterisk in Figure 3.7. The definition of a flux profile has been made in this work using only the more numerous manganese measurements made on the front face. The fission-rate attenuation in the z direction through the plate is assumed independent of X,Y position, allowing a considerable simplification of the treatment with little loss of accuracy. To support this assumption it is noted that the average difference in the ratios of back to front manganese measurement is less than 3% between the central position of the plate and the edge of the plate.

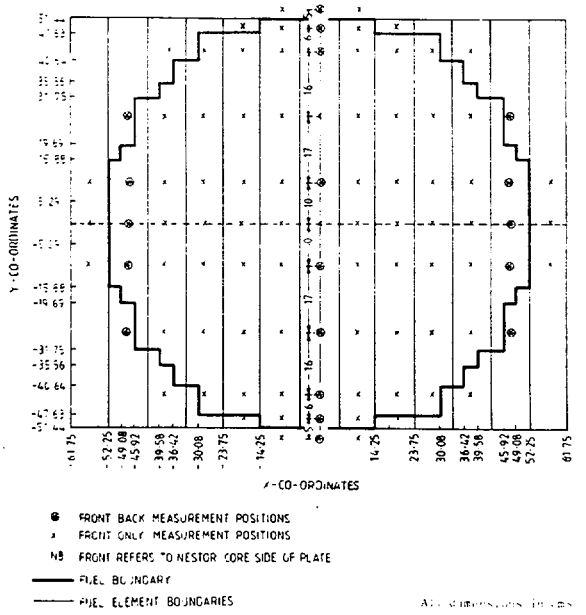

Figure 3.7 *Fuel element configuration & manganese foil measurement positions*

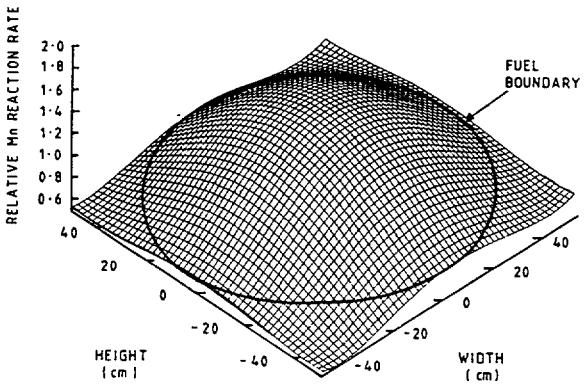

Figure 3.8 *NESDIP 2 fission plate source profile*

The manganese reaction-rate measurements on the front face of the plate were input to the CRISP code (2) to define the manganese reaction-rate surface covering the plate. The surface fit is shown in Figure 3.8. From this surface the average manganese reaction-rate within the elements of any source mesh overlaid onto the fission plate can be defined. To model exactly the boundaries of the plate and to provide adequate spatial resolution, the source mesh shown in Figure 3.9 was used. The fractional uncertainty on the mean manganese reaction-rate in each source mesh due to the surface fitting and integration is taken as 2%.

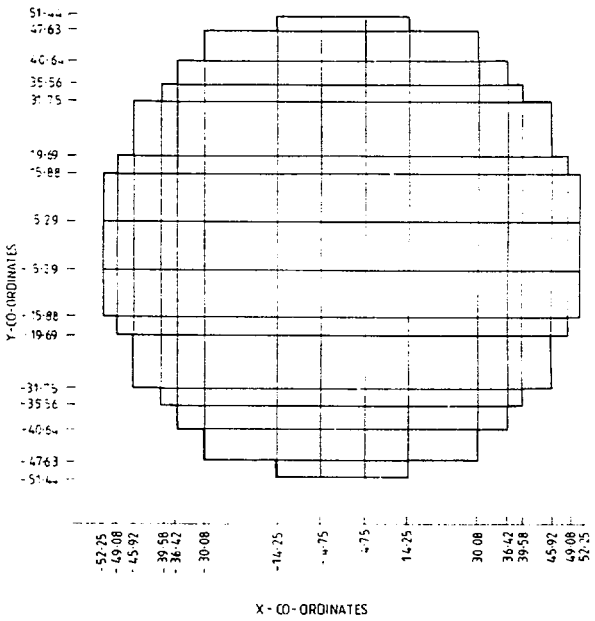

Figure 3.9 *Source mesh boundaries*

3.2.3 The Distribution of U235 in the Fuel

The fission plate used in the REPLICA experiment used similar fuel strips to those used in the NESDIP fission plate. During the REPLICA experiment a sample of 23mm long sections taken from fuel strips were analysed for U235 content by measurement, with a Ge(Li) detector, of the U235 185keV natural decay line. The standard deviation on the 23 measurements was 2%. Unlike the REPLICA experiment the mesh required to define the neutron source for calculational analysis does not contain elements of a single size (see Figure 3.9). The uncertainty on U235 content (and hence the power) in each mesh is therefore dependent on mesh size. The uncertainty on U235 content in a mesh containing N 23mm long fuel sections is $\sqrt{2^2/N}\,\%$. Due to the large number of small meshes near the periphery of the fission plate the average number of 23mm long fuel-sections in each source mesh is only 11, whereas at the centre of the plate the value is about 29.

The large number of source meshes defined (225 in total) makes the uncertainty of the total plate power insensitive to uncertainty on U235 content in each mesh. For this reason the uncertainty on the U235 content in each mesh has been derived using N = 11 at

$$\sqrt{\frac{2^2}{11}} = 0.6\%$$

3.2.4 The Fission-Rate Profile

The fission-rate profile in X and Y is taken as the manganese reaction-rate profile on the front face of the fuel plate, as shown in Figure 3.8. In the definition of the fission-rate in each mesh the z dependence is irrelevant provided it is independent of X and Y. This assumption has been made and justified in Section 3.2.2. The uncertainty estimate on the average fission-rate in each source mesh combined the uncertainty of the surface fitting and integration procedures of CRISP and the uncertainty on the U235 content, i.e.

$$(2^2 + 0.6^2)^{1/2} = 2.1\%$$

It has become customary to provide a spatial neutron source definition which integrates to a total plate power of 1 Watt. Table 3.2 contains neutron source distribtions, both rectangular and annular for the NESDIP plate in the NESDIP 2 array; constants of 3.121,10 fissions per Watt and 2.437 neutrons per fission have been used in its derivation.

3.2.5 The Z Dependence of the Fission-Rate Distribution

The relative fission rates in the two layers of fuel contained within the plate have been derived from measurements performed to establish the absolute power of the plate. This is discussed in the next section, suffice to say that the average fission rate ratio between the front and back fuel spike was 1.044 ± 0.015.

3.2.6 The Absolute Calibration of the Fission Plate

The absolute power in the fission plate, expressed per NESTOR watt, has been determined by combining measurements of absolute fission-rate at spot values, gained by decay product counting, with the fission-rate profile data derived in CRISP.

To obtain absolute measurements of the fission-rate within the NESDIP plate the central fuel element was replaced by a demountable unirradiated fuel element in which the 2 central fuel strips had six 0.75″ diameter fuel discs located in trepanned holes. The arrangement is shown in Figure 3.10. The fission plate was irradiated at a NESTOR power of 15kW for 45 minutes and the six discs removed for fission product counting. The fission product counting provides a direct measure of the fission-rate within the fuel; the fission-rates per disc are given in Table 3.3. Also tabulated are the spot values of manganese reaction-rate on the front face of the plate directly over the fuel disc locations. The average fission-rate per disc per unit manganese reaction-rate, derived from the three axial locations is P fissions.sec^{-1} per dps.atom^{-1} with a standard deviation of 0.7%. To this must be incorporated a systematic uncertainty of 3% to account for the uncertainties in the counting of the fission product activity (i.e. detector efficiency, gamma-ray escape probability from the sample and long lived activity in the fuel) and for the uncertainty in the subsequent analysis used to obtain the fission-rates (i.e. fission product yield of Ba, and the branching ratio for the La140 decay scheme).

The manganese rection-rate averaged over the X-Y profile has been evaluated at Q ±0.3% dps/atom per NESTOR Watt (using an uncertainty of 2.1% on each source mesh). The average fission-rate per cm^3 over the whole plate per NESTOR Watt, $\bar{F}$, can be evaluted from:

$$\bar{F} = \frac{P\,(3.1\%)}{V_D\,(1\%)} \times Q\ (0.3\%) \qquad \ldots\ldots 1$$

where V_D is the volume of a single 1mm thick, 0.75″ diameter fuel disc = 0.2850 cm^3

$$= S\ (3.3\%)\ \frac{\text{Fission.cm}^{-3}.\text{S}^{-1}}{\text{NESTOR Watt}}$$

To obtain a power of 1 Watt in the plate the value of $\bar{F}$ should equate to

$$\frac{F_o}{V_p} = T\ \frac{\text{Fissions.cm}^{-3}.\text{s}^{-1}}{\text{Plate Watt}} \qquad \ldots\ldots 2$$

where F_o = 3.121,10 fissions.Watt^{-1}

V_p is the volume of the fuelled region in the fission plate = 8.681,3 cm^3

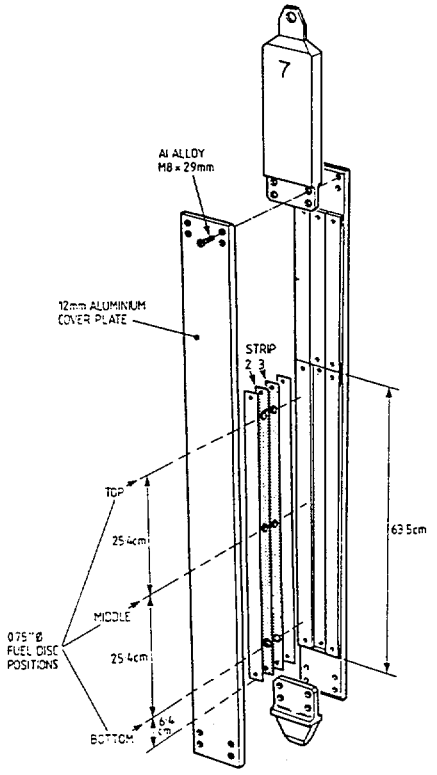

Figure 3.10 *Location of fission discs in fuel element*

Subdivision of Equation *1* by Equation *2* yields the ratio R between plate power and NESTOR power, i.e.:

$$R = \frac{S}{T}$$

$$= XXXXX\ (3.3\%)\ \frac{\text{Plate Watts}}{\text{NESTOR Watt}}$$

This analysis assumes a continuous distribution of fuel over the area of the fission plate. In practice clearance gaps between the fuel elements and betweens the individual fuel strips in each element dilute the fuel content. To correct for this dilution a factor of 0.963 ± 1% has to be applied to R. Hence we find that the fission plate power per NESTOR Watt, R,

is XXXXX (3.3%) x 0.963 (1%)

= XXXXX (3.5%) Watts

Table 3.3 Fission-rate measurements and their comparison with extrapolated manganese reaction-rates

	Fission-Rate per Disc [Fission.sec^{-1} per Disc / NESTOR Watt]			Manganese Reaction-Rate at Disc Position Derived from CRISP [dps.atom^{-1} / NESTOR Watt]	Mean Fission-Rate per Disc CRISP Manganese Point Values
			Mean		
Position*	Strip 2*	Strip 3*	Strip 1 & 2		
Top	XXXXX	XXXXX	XXXXX	XXXXX	XXXXX
Middle	XXXXX	XXXXX	XXXXX	XXXXX	XXXXX
Bottom	XXXXX	XXXXX	XXXXX	XXXXX	XXXXX
					Mean = XXXXX
					S.d. = XXXXX

*See Figure 3.10

4 · Threshold reaction-rate measurements

Three fast neutron threshold reactions have been measured along the nuclear axis of the shields. They are the S32(n,p)P32, In115(n,n')In115m and Rh103(n,n')Rh103m reactions. The rhodium reaction-rate was measured over four decades of attenuation through the water cell, RPV and into the cavity. For measurements in the RPV region 0.6cm air gaps were opened up between the slab components to allow the insertion of the activation detectors. The indium and sulphur measurements were made in the RPV region and the cavity. In addition, during all irradiations of activation detectors within the shields, three sulphur pellets were placed in locations at the centre of the front face of the fission plate to monitor its run to run power via the S32(n,p)P32 reaction. Off-axis scans were also made in the cavity using the sulphur detectors to demonstrate the axial profile of the fast neutron flux.

4.1 Rhodium Activation Measurements

The rhodium measurements were made under cadmium to reduce impurity activation. The foils were located within the water cells on a thin perspex jig which was sprung against the cell wall. The positional uncertainty was 1mm. In the RPV and cavity the foils were located on a thin aluminium carrier. The uncertainties associated with the calibration of the NaI spectrometer counting system is 3%.

4.2 Sulphur Activation Measurements

In the RPV and cavity 20g sulphur samples were located on thin aluminium carriers. To facilitate their inclusion in the RPV, 0.6cm voids were introduced between the 5.1cm thick mild steel components. The activated sulphur is first slowly burnt in a thin aluminium cup which is subsequently collapsed to a disc. The residue containing the P32 activity is then counted. The calibration of the counting system including counter efficiency, losses due to burning, and reference data has a systematic uncertainty of 4%.

4.3 Indium Activation Measurements

The indium samples were located on the thin aluminium carrier in the RPV and Cavity. The calibration of the counting system for these foils, including Ge(Li) efficiency and reference data has a systematic uncertainty of 2%.

4.4 Activation Results

The reaction-rates, uncorrected for the contribution due to NESTOR core neutrons, measured along the nuclear axis in the NESDIP 1 and 2 arrays are shown in Tables 4.1 and 4.2 respectively. The NESTOR core neutron contributions are discussed in Section 4.6. The foil irradiation locations are common to both arrays and are defined in Figure 4.1.

The comparison of the axial scans using the sulphur detectors in both the NESDIP 1 and 2 cavities is made in Table 4.3 and Figure 4.2.

4.5 Perturbation in the RPV Region

The RPV region is constructed from four 5.1cm thick mild steel plates and the rear wall of the water cell. To obtain activation measurements through the RPV region four air gaps of 0.6cm were opened up between these components. The perturbation of activation measurements made 4cm into the cavity due to the introduction of these voids is given in Table 4.4 (note that the measurements were made at a constant distance from the rear face of the RPV region irrespective of whether the RPV plates were separated by air gaps or closed up). The anomalous result in Table 4.4 is that for sulphur in the NESDIP 1 configuration. The timescales imposed on this work has not allowed further experimentation to be completed in order to resolve this discrepancy. Repeat measurements will be made when the configuration is rebuilt in ASPIS but until then the discrepancy will remain unresolved. The remainder of the ratios suggest a slight reduction in measured reaction-rates caused by opening the plates as would be expected.

4.6 Core Background Corrections

A small fraction of neutrons present in the arrays originate from leakage from the NESTOR core. This background has been estimated in the cavity region from measurements by a hydrogen filled proportional counter with the boral cave shutter both open and shut. The boral shutter, to a first approximation, shuts down the fission plate leaving only fast neutron leakage from the NESTOR core. In the cavity, at measurement reference position 18, the shutter closed signal is 4% of the shutter open signal. This value is entirely consistent with measured values in the REPLICA experiment.

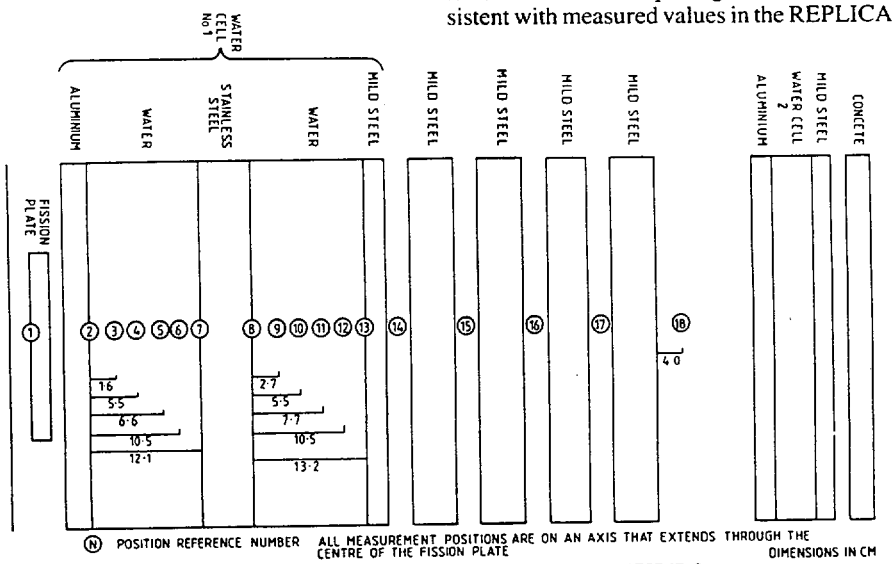

Figure 4.1 *Measurement locations in the NESDIP 1 and NESDIP 2 arrays*

Recent work (3), conducted to study the true shutdown factor of the plate power when the boral shutters are closed, has led to modification of this backgrouind correction to $(2 \pm 1)\%$.

The background correction of 2% applies in both the RPV and cavity regions. In the water cells the value of $(1 \pm 1)\%$ is appropriate.

Table 4.1 Measured reaction-rates through the NESDIP 1 radial shield

Reference Location	Position*	Reaction-Rates+ (dps.atom^{-1} per NESTOR Watt)		
		Rh103(n,n')Rh103m Systematic ± 3%	In115(n,n')In115m Systematic ± 2%	S32(n,p)P32 Systematic ± 4%
Monitor	1	–	–	XXXXX ±0.3%
Front Compartment of Water Cell No 1	2	XXXXX ±0.1%	–	–
	4	XXXXX ±0.2%	–	–
	6	XXXXX ±0.3%	–	–
Rear Compartment of Water Cell No 1	8	XXXXX ±0.6%	–	–
	10	XXXXX ±1.7%	–	–
	12	XXXXX ±2.3%	–	–
RPV	14	XXXXX ±2.2%	XXXXX ±0.6%	XXXXX ±0.4%
	15	XXXXX ±2.5%	XXXXX ±1.4%	XXXXX ±0.5%
	16	–	XXXXX ±1.7%	XXXXX ±0.5%
	17	XXXXX ±3.5%	XXXXX ±1.9%	XXXXX ±0.6%
Cavity	18	XXXXX ±4.0%	XXXXX ±6.4%	XXXXX ±5.0%

*Reference Figure 4.1
+ Reaction-rates are as measured. No background correction has been applied.
XXXXX denotes measurement

Table 4.2 Measured Reaction-rates through the NESDIP 2 radial shield

Reference Location	Position*	Reaction-Rates+ (dps.atom^{-1} per NESTOR Watt)		
		Rh103(n,n')Rh103m Systematic ± 3%	In115(n,n')In115m Systematic ± 2%	S32(n,p)P32 Systematic ± 4%
Monitor	1	–	–	XXXXX ±1%
Front Compartment of Water Cell No 1	2	XXXXX ±0.1%	–	–
	3	XXXXX ±0.2%	–	–
	4	XXXXX ±0.3%	–	–
	5	XXXXX ±0.3%	–	–
	6	XXXXX ±0.5%	–	–
	7	XXXXX ±0.5%	–	–
Rear Compartment of Water Cell No 1	8	XXXXX ±0.9%	–	–
	9	XXXXX ±0.8%	–	–
	10	XXXXX ±1.7%	–	–
	11	XXXXX ±1.7%	–	
	12	XXXXX ±3.1%	–	–
	13	XXXXX ±2.4%	–	–
RPV	14	XXXXX ±2.0%	XXXXX ±1.0%	XXXXX ±2%
	15	XXXXX ±2.0%	XXXXX ±0.9%	XXXXX ±3%
	16	XXXXX ±3.0%	XXXXX ±1.5%	XXXXX ±2%
	17	XXXXX ±3.5%	XXXXX ±1.7%	XXXXX ±2%
Cavity	18	XXXXX ±4.0%	XXXXX ±2.0%	XXXXX ±2%

*Reference Figure 4.1
+ Reaction-rates are as measured. No background correction has been applied.
XXXXX denotes measurement

Table 4.3 S32(n,p)P32 Reaction-rate profile in the cavity*

Distance from Nuclear Centre+ cm	Reaction-Rate (dps.atom^{-1} per NESTOR Watt)		Profile (Normalised to 1.0 at Nuclear Centre)	
	NESDIP 1	NESDIP 2	NESDIP 1	NESDIP 2
+75		XXXXX		0.15
+50	XXXXX	XXXXX	0.22	0.44
+25	XXXXX	XXXXX	0.67	0.86
0	XXXXX	XXXXX	1.0	1.0
−25	XXXXX	XXXXX	0.65	0.83
−50	XXXXX	XXXXX	0.27	0.45
−75	—	XXXXX	—	0.13

*Measurements made on a vertical axis intersecting the nuclear centre of the trolley and 4cm off the front wall of the cavity

+ Nuclear centre is 88.9cm from the floor of the trolley

XXXXX denotes measurement

Table 4.4 Comparison of activation measurements in the cavity with the RPV plates open and closed

Reaction	Reaction-Rate Ratio (Plates Open/ Plates Closed)	
	NESDIP 1	NESDIP 2
Rh103(n,n')Rh103m	0.95±0.05	0.98±0.04
In115(n,n')In115m	0.92±0.07	0.95±0.04
S32(n,p)P32	1.13±0.03	0.98±0.03

Figure 4.2 *Relative S32 (n,p) P32 reaction-rate axial profiles in the cavity of the NESDIP 1 and NESDIP 2 arrays*

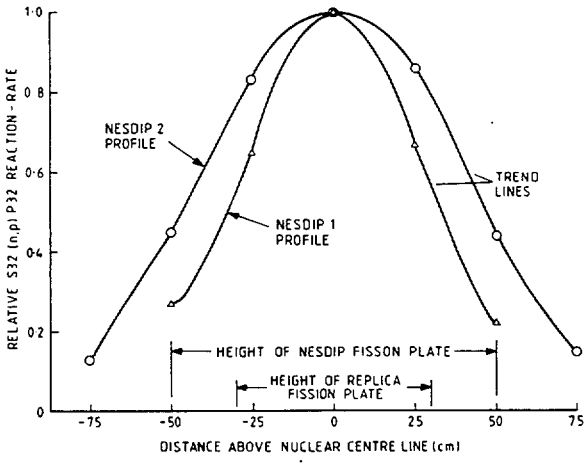

The differential neutron energy spectrum has only been measured in the cavity of the NESDIP 2 array. The measurement position was located 4cm off the face of the cavity and centred on the nuclear axis (position reference number 18). The air gaps described in Section 4.5 were included inbetween the plates of the RPV region during these measurements.

The measurements were made with 3 hydrogen-filled proportional counters and a NE213 organic liquid scintillator. The proportional counters were filled to pressures of 1, 3 and 10 atmospheres. The proton recoil spectra were analysed using the SPEC(4) and NE213(5) codes.

The high energy portion of the spectrum derived for the NE213 proton recoil data was normalised using the measured S32(n,p)P32 reaction-rate at the measurement location. The resulting neutron spectrum is given in Table 5.1 and Figure 5.1.

Energy Upper Boundaries (MeV)	Flux per Unit Lethargy (n.cm^{-2}.s^{-1})	Energy Upper Boundaries (MeV)	Flux per Unit Lethargy (n.cm^{-2}.s^{-1})
1.0000E+01	XXXXX	5.6416E−01	XXXXX
8.8250E+00	XXXXX	4.9787E−01	XXXXX
7.7880E+00	XXXXX	4.3937E−01	XXXXX
6.8729E+00	XXXXX	3.8774E−01	XXXXX
6.0653E+00	XXXXX	3.4218E−01	XXXXX
5.3526E+00	XXXXX	3.0197E−01	XXXXX
4.7237E+00	XXXXX	2.6649E−01	XXXXX
4.1686E+00	XXXXX	2.3518E−01	XXXXX
3.6788E+00	XXXXX	2.0754E−01	XXXXX
3.2465E+00	XXXXX	1.8316E−01	XXXXX
2.8651E+00	XXXXX	1.6164E−01	XXXXX
2.5284E+00	XXXXX	1.4264E−01	XXXXX
2.2313E+00	XXXXX	1.2588E−01	XXXXX
1.9691E+00	XXXXX	1.1109E−01	XXXXX
1.7377E+00	XXXXX	9.8037E−02	XXXXX
1.5336E+00	XXXXX	8.6517E−02	XXXXX
1.3534E+00	XXXXX	7.6351E−02	XXXXX
1.1943E+00	XXXXX	6.7380E−02	XXXXX
1.0540E+00	XXXXX	5.9462E−02	XXXXX
9.3015E−01	XXXXX	5.2475E−02	XXXXX
8.2085E−01	XXXXX	4.6309E−02	XXXXX
7.2440E−01	XXXXX	4.0868E−02	XXXXX
6.3928E−01	XXXXX	3.6066E−02	XXXXX

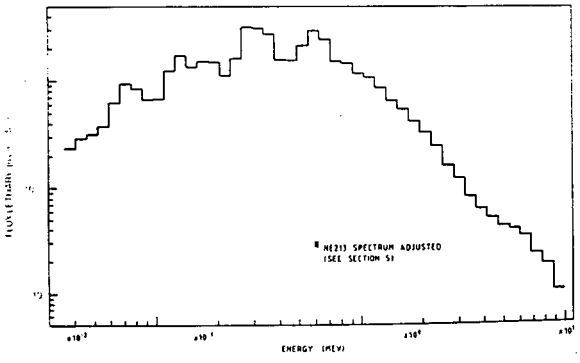

Figure 5.1 *Neutron energy spectrum measured in the cavity of the NESDIP 2 array*

6 Monte Carlo calculations

The analysis of both the NESDIP 1 and 2 shield configurations has been performed using versions 3.1 of the Monte Carlo code MCBEND (6). The skeleton of this section has been included in this report as an aid to the calculator. The results will be given in the second edition of the paper.

6.1 The Geometric Model

A precise geometric representation of the NESDIP 1 and 2 radial shield configurations in the ASPIS trolley was achieved using the combinatorial geometry package of MCBEND. The calculational models are shown in Figures 6.1 and 6.2.

The only approximation in the model is the exclusion of the 0.6cm wide voids between the mild steel plates in the RPV region. It is assumed from the evidence presented in Section 4.5 that the activation rates in the cavity are insensitive to the presence of the voids between the plates.

6.2 The Fission Plate Source Distributions

The derivations of the source distributions for the two fission plates has been described in detail in Section 3. The Z dependence of the source between the 2 fuel strips in the NESDIP plate has not been modelled and a uniform source across the thickness of the plate has been used. The effect of this approximation on the calculated fluxes is trivial but it does allow a halving of the source regions required to 225. The Z dependence of the source in the REPLICA plate has been modelled assuming the measured profile given in the REPLICA report.

The output from the fission plate source derivation program CRISP is formatted in accordance with the input requirements for the source module in MCBEND and has been included directly into the input data stream.

The fission neutron energy spectrum for U235 due to Story and Miller (7) has been used in this analysis.

6.3 The Scoring Data

Scoring is in rectangular regions having a 20cm x 20cm cross-sectional area and 2mm depth. The regions are centred on the measurement positions through the shield which have been defined in Figure 4.1. The group fluxes were scored in a 27 energy group structure with a lower energy cut-off at 0.11MeV.

6.4 Nuclear Data and Material Definitions

The UK Nuclear data library (UKNDL), in a 8000-group structure, has been used as the source for the transmission cross-sections. The use of the 8000 group data represents a departure from the usual use of the 300g version. In the REPLICA report a comparison of the calculated reaction-rate was made between analyses conducted using the 300 and 8000 group data. The findings of this study are summarised in Table 6.1. The calculated Rh103(n,n')Rh103m and In115(n,n')In115m reaction-rates demonstrate complete agreement between the use of the two data sets. A slight bias is detected for the S32(n,p)P32 reaction with the 8000 group data calculation generally underpredicting the 300 group data calculation by some 6%.

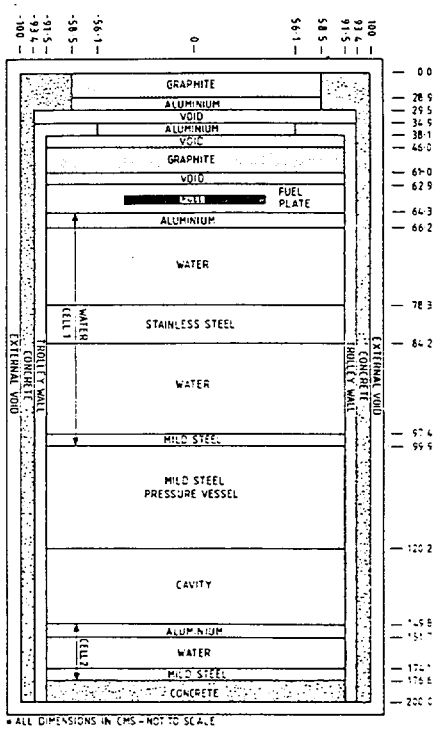

Figure 6.1 *MCBEND model of the NESDIP 1 array*

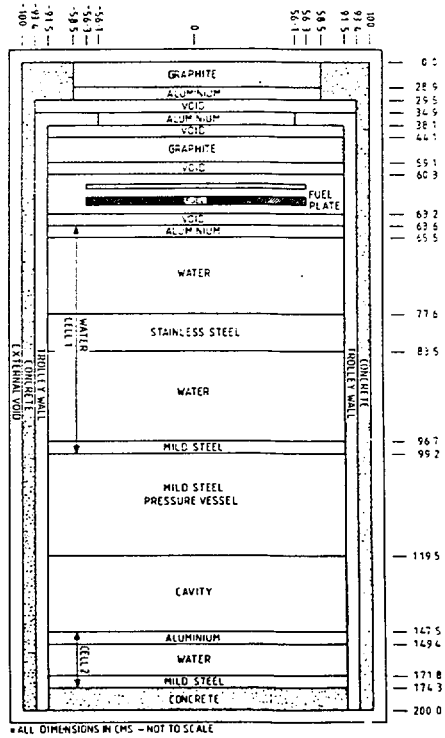

Figure 6.2 *MCBEND model of the NESDIP 2 array*

The response cross-sections have been taken from the International Reactor Dosimetry File (8). They have been included in the 620 energy-group structure.

6.5 Acceleration for the Monte Carlo Calculations

The finite-element diffusion code FENDER (9) has been used to derive a spatial and energy dependent importance function for use in accelerating the MCBEND calculations. The technique involves an adjoint solution of the diffusion equation for the shield configuration with the adjoint source located at the scoring position of interest for the MCBEND calculation. Because of the similarities between the NESDIP 1 and NESDIP 2 shields the same importance map has been used in both cases. The finite-element mesh used to define the importance map is an RZ system and is detailed in Figure 6.3.

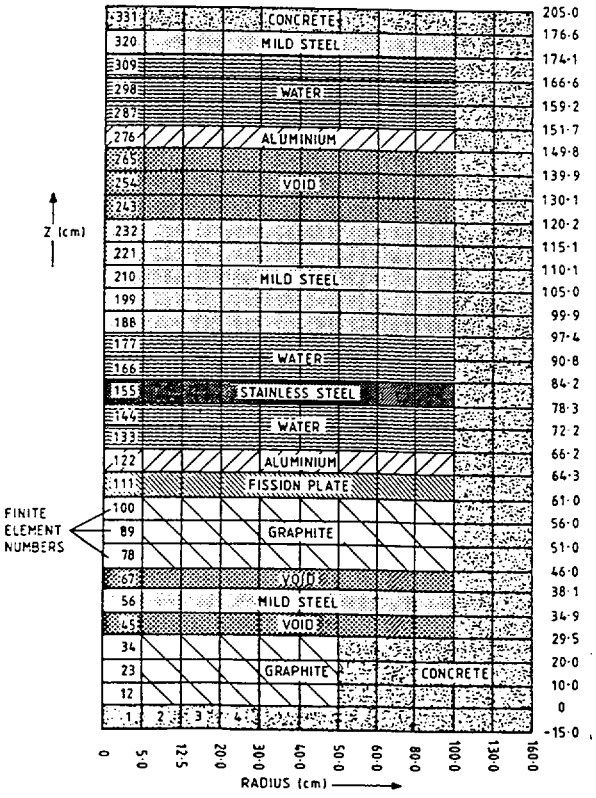

Figure 6.3 *FENDER mesh description*

6.6 Monte Carlo Results

For the NESDIP 1 case 195000 particles were tracked and the calculated reaction-rates per plate Watt are given in Table 6.2. For the NESDIP 2 case 570000 particles were tracked and the calculated reaction-rates are given in Table 6.3.

6.7 Adjustments to the Experimental and Calculated Reaction-Rates

The comparison of experimental and calculated reaction-rates is to be made for a NESTOR power of 1 Watt and is to consider only neutrons which had their source in the fission plate. To achieve this three adjustments have to be made:

(1) To remove from the measured reaction-rates that component which is due to the NESTOR core background. This has been discussed in Section 4.6 and has been established as a 2% reduction in the RPV and Cavity and a 1% reduction in the Water Cells for both the NESDIP 1 and NESDIP 2 arrays.

(2) To correct for the size of the Monte Carlo scoring regions compared to the size of the measurement foils. The ratio of axial/mean fluxes over the Monte Carlo scoring regions varies slightly with energy and position. For the NESDIP 1 calculation the ratio of 1.04 ± 1% derived for the REPLICA experiment has been used. The ratio from the NESDIP 2 calculation has been determined from the axial measurements of the S32(n,p)P32 reaction in the cavity already shown in Table 4.3. A cosine distribution of width 140cm has been fitted to the measured profile and from this the axial to mean ratio of 1.014 for the S32(n,p)P32 reaction-rate has been derived with an uncertainty of 1%. This ratio is assumed to apply for all reactions.

(3) To normalise the calculation to 1 NESTOR watt. The fission-plate calibrations detailed in Section 3 give the fission plate powers per NESTOR Watt for the REPLICA and NESDIP fission plates in the NESDIP 1 and 2 arrays as XXXXX ±4.0% and XXXXX ±3.5% Watts respectively.

6.8 Comparison of Calculation with Experiment

In Tables 6.4 and 6.5 the calculated and experimental reaction-rates, each adjusted as described in Section 6.7, are compared.

Table 6.1 *A comparison of reaction-rates calculated in the Replica using 300 and 8000 group data from UKNDL*

Position	Response Calculated Using 8000 Group Data / Response Calculated Using 300 Group Data		
	Rh103(n,n')Rh103m	**In115(n,n')In115m**	**S32/n,p)P32**
A3	1.01 ±0.05	0.99 ±0.04	0.93 ±0.03
A4	0.98 ±0.04	0.97 ±0.04	0.92 ±0.03
A6	0.96 ±0.04	0.96 ±0.04	0.94 ±0.04
A7	1.00 ±0.03	1.03 ±0.04	0.97 ±0.04

Table 6.2 Responses calculated for the NESDIP 1 array

Location	Measurement Position Reference Number	MCBEND Zone Number	Reaction-Rates (dps.atom^{-1} per Plate Watt)						Flux > 0.1MeV (n.cm^{-2}.s^{-1} per Plate Watt)
			A127(n,A)Na24	Rh103(n,n')Rh103m	In115(n,n')In115m	S32(n,p)P32	ASTM 800 Steel	Fe54(n,p)Mn54	
Monitor	1	29	XXXXX ±2%	XXXXX ±6%	XXXXX ±3%	XXXXX ±2%	XXXXX ±9%	XXXXX ±2%	XXXXX ±19%
Front	2	30	XXXXX ±2%	XXXXX ±5%	XXXXX ±3%	XXXXX ±2%	XXXXX ±9%	XXXXX ±2%	XXXXX ±13%
Water	4	31	XXXXX ±2%	XXXXX ±6%	XXXXX ±4%	XXXXX ±2%	XXXXX ±11%	XXXXX ±2%	XXXXX ±21%
Compartment	6	32	XXXXX ±3%	XXXXX ±11%	XXXXX ±5%	XXXXX ±3%	XXXXX ±13%	XXXXX ±3%	XXXXX ±40%
Rear	8	33	XXXXX ±4%	XXXXX ±6%	XXXXX ±4%	XXXXX ±3%	XXXXX ±7%	XXXXX ±3%	XXXXX ±10%
Water	10	34	XXXXX ±4%	XXXXX ±4%	XXXXX ±3%	XXXXX ±3%	XXXXX ±4%	XXXXX ±3%	XXXXX ±7%
Compartment	12	35	XXXXX ±4%	XXXXX ±3%	XXXXX ±4%	XXXXX ±3%	XXXXX ±3%	XXXXX ±3%	XXXXX ±5%
	13	36	**XXXXX ±4%**	**XXXXX ±4%**	**XXXXX ±4%**	**XXXXX ±3%**	**XXXXX ±4%**	**XXXXX ±3%**	**XXXXX ±6%**
RPV	14	37	XXXXX ±4%	XXXXX ±4%	XXXXX ±4%	XXXXX ±3%	XXXXX ±3%	XXXXX ±3%	XXXXX ±4%
	15	38	XXXXX ±4%	XXXXX ±3%	XXXXX ±3%	XXXXX ±3%	XXXXX ±3%	XXXXX ±3%	XXXXX ±4%
	16	39	XXXXX ±4%	XXXXX ±3%	XXXXX ±3%	XXXXX ±3%	XXXXX ±3%	XXXXX ±3%	XXXXX ±4%
	17	40	XXXXX ±4%	XXXXX ±3%	XXXXX ±4%	XXXXX ±4%	XXXXX ±3%	XXXXX ±4%	XXXXX ±4%
Cavity	–	41	XXXXX ±4%	XXXXX ±5%	XXXXX ±8%	XXXXX ±4%	XXXXX ±4%	XXXXX ±4%	XXXXX ±4%
	18	42	XXXXX ±4%	XXXXX ±5%	XXXXX ±8%	XXXXX ±4%	XXXXX ±4%	**XXXXX ±4%**	XXXXX ±4%
	–	43	XXXXX ±6%	XXXXX ±7%	XXXXX ±6%	XXXXX ±6%	XXXXX ±9%	XXXXX ±6%	XXXXX ±11%

Table 6.3 Responses calculated for the NESDIP 2 array

Location	Measurement Position Reference Number	MCBEND Zone Number	Reaction-Rates (dps.atom^{-1} per Plate Watt)						Flux > 0.1MeV (n.cm^{-2}.s^{-1} per Plate Watt)
			A127(n,A)Na24	Rh103(n,n')Rh103m	In115(n,n')In115m	S32(n,p)P32	ASTM 800 Steel	Fe54(n,p)Mn54	
Front	2	30	XXXXX ±2%	XXXXX ±4%	XXXXX ±2%	XXXXX ±2%	XXXXX ±6%	XXXXX ±2%	XXXXX ±13%
Water	3	31	XXXXX ±2%	XXXXX ±4%	XXXXX ±3%	XXXXX ±2%	XXXXX ±5%	XXXXX ±2%	XXXXX ±10%
Compartment	4	32	XXXXX ±2%	XXXXX ±4%	XXXXX ±4%	XXXXX ±2%	XXXXX ±26%	XXXXX ±2%	XXXXX ±44%
	5	33	XXXXX ±2%	XXXXX ±5%	XXXXX ±4%	XXXXX ±2%	XXXXX ±6%	XXXXX ±2%	XXXXX ±18%
	6	34	XXXXX ±2%	XXXXX ±3%	XXXXX ±3%	XXXXX ±2%	XXXXX ±5%	XXXXX ±2%	XXXXX ±10%
	–	35	XXXXX ±3%	XXXXX ±5%	XXXXX ±5%	XXXXX ±3%	XXXXX ±5%	XXXXX ±3%	XXXXX ±7%
Rear	8	36	XXXXX ±3%	XXXXX ±4%	XXXXX ±4%	XXXXX ±3%	XXXXX ±5%	XXXXX ±2%	XXXXX ±9%
Water	9	37	XXXXX ±3%	XXXXX ±4%	XXXXX ±3%	XXXXX ±3%	XXXXX ±4%	XXXXX ±3%	XXXXX ±7%
Compartment	10	38	XXXXX ±3%	XXXXX ±3%	XXXXX ±3%	XXXXX ±3%	XXXXX ±3%	XXXXX ±3%	XXXXX ±5%
	11	39	XXXXX ±3%	XXXXX ±3%	XXXXX ±3%	XXXXX ±3%	XXXXX ±3%	XXXXX ±2%	XXXXX ±4%
	12	40	XXXXX ±3%	XXXXX ±3%	XXXXX ±3%	XXXXX ±3%	**XXXXX ±3%**	**XXXXX ±2%**	**XXXXX ±4%**
	13	41	XXXXX ±3%	XXXXX ±3%	XXXXX ±3%	XXXXX ±3%	XXXXX ±3%	XXXXX ±3%	XXXXX ±4%
RPV	14	42	XXXXX ±3%	XXXXX ±3%	XXXXX ±3%	XXXXX ±3%	XXXXX ±3%	XXXXX ±3%	XXXXX ±3%
	15	43	XXXXX ±3%	XXXXX ±2%	XXXXX ±3%	XXXXX ±3%	XXXXX ±2%	XXXXX ±3%	XXXXX ±3%
	16	44	XXXXX ±3%	XXXXX ±2%	XXXXX ±3%	XXXXX ±3%	XXXXX ±2%	XXXXX ±3%	XXXXX ±3%
	17	45	XXXXX ±3%	XXXXX ±2%	XXXXX ±3%	XXXXX ±3%	XXXXX ±2%	XXXXX ±3%	XXXXX ±3%
Cavity	18	46	XXXXX ±3%	XXXXX ±3%	XXXXX ±3%	XXXXX ±3%	XXXXX ±3%	XXXXX ±3%	XXXXX ±3%
		47	XXXXX ±4%	XXXXX ±4%	XXXXX ±5%	XXXXX ±7%	XXXXX ±4%	XXXXX ±8%	XXXXX ±5%

Table 6.4 Comparison of calculated and measured reaction-rates in the NESDIP 1 array

Location	Measurement Position Reference Number*	MCBEND Zone Number	Calculated to Measured Reaction-Rate Ratios (c/m)		
			Rh103(n,n')Rh103m	In115(n,n')In115m	S32(n,p)P32
Monitor	1	29	–	–	XXXXX±0.06
Front	2	30	XXXXX±0.07	–	–
Water	4	31	XXXXX±0.07	–	–
Compartment	6	32	XXXXX±0.12	–	–
Rear	8	33	XXXXX±0.07	–	–
Water	10	34	XXXXX±0.06	–	–
Compartment	12	35	XXXXX±0.06	–	–
RPV	14	37	XXXXX±0.07	XXXXX±0.07	XXXXX±0.08
	15	38	XXXXX±0.07	XXXXX±0.07	XXXXX±0.08
	16	39	–	XXXXX±0.07	XXXXX±0.08
	17	40	XXXXX±0.07	XXXXX±0.07	XXXXX±0.07
Cavity	18	42	XXXXX±0.08	XXXXX±0.12	XXXXX±0.09

*Reference Figure 4.1

Table 6.5 Comparison of calculated and measured reaction-rates in the NESDIP 2 array

Location	Measurement Position Reference Number*	MCBEND Zone Number	Calculated to Measured Reaction-Rate Ratios (c/m)		
			Rh103(n,n')Rh103m	In115(n,n')In115m	S32(n,p)P32
Front	2	30	XXXXX±0.06	—	—
Water	3	31	XXXXX±0.06	—	—
Compartment	4	32	XXXXX±0.14	—	—
	5	33	XXXXX±0.07	—	—
	6	34	XXXXX±0.06	—	—
	7	35	XXXXX±0.06	—	—
Rear	8	36	XXXXX±0.06	—	—
Water	9	37	XXXXX±0.06	—	—
Compartment	10	38	XXXXX±0.06	—	—
	11	39	XXXXX±0.06	—	—
	12	40	XXXXX±0.06	—	—
	13	41	XXXXX±0.06	—	—
RPV	14	42	XXXXX±0.06	XXXXX±0.06	XXXXX±0.07
	15	43	XXXXX±0.06	XXXXX±0.06	XXXXX±0.08
	16	44	XXXXX±0.06	XXXXX±0.06	XXXXX±0.07
	17	45	XXXXX±0.07	XXXXX±0.06	XXXXX±0.07
Cavity	18	46	XXXXX±0.06	XXXXX±0.05	XXXXX±0.07

*Reference Figure 4.1

7 Summary

This document describes the ASPIS-PCA slab geometry benchmark experiments carried out as part of the NESTOR Shielding and Dosimetry Improvement Programme, NESDIP. The configurations are based upon the 12/13 radial shield geometry of the ORNL PCA and AEEW PCA-REPLICA. The lateral dimensions, however, are increased and the configurations are more amenable to analysis using one- or two-dimensional geometry codes.

Full description of the experimental configurations are given including the source definitions and a summary of measurements. The intention is that the benchmarks should be used as blind tests of methods of calculation and data used in the analysis of LWR radial shields. Accordingly neither the absolute calibration of the source nor the detector responses are given. These will be incorporated into the second edition of the paper which will also include an analysis using the Monte Carlo code MCBEND

8 References

1 The PCA Replica Experiment PART 1. Winfrith Measurements and Calculations
AEEW - R 1736.

2 Curl I J
CRISP - A Computer Code to Define Fission-Plate Source Profiles
RPD/IJC/934 Internal UKAEA Document.

3 Carter M D
ASPIS: Correction for NESTOR Core Background
RPD/MDC/1048 Internal UKAEA Document.

4 Benjamin P W, Kemshell P W, Brickstock A
The Analysis of Proton Recoil Spectra
AWRE 0-9/68

5 Grimstone M J
The RADAK Users Manual
AEEW - M 1455

6 MCBEND Users Guide
UKAEA Document. ANSWERS/MCBEND

7 Story J S and Miller P C
Fission Neutron Spectra for Shielding Calculations
Internal UKAEA Document.

8 Cullen D E, Kochrov N and McLaughlin
The International Reactor Dosimetry File (IRDF-82)
IAEA-NDS-41/R

9 Shuttleworth E
FENDER - A Finite Element Code for the Solution of the Diffusion Equation in Shield Design Applications
Annals of Nuclear Energy, Vol 8 pp 597 to 607, 1981.

10 Butler J
The NESTOR Shielding and Dosimetry Improvement Programme for PWR Applications
PRPWG/P(82)5 Internal UKAEA Document